Am. J. Hum. Genet. 75:267–281, 2004

High-Resolution Molecular Characterization of 15q11-q13 Rearrangements by Array Comparative Genomic Hybridization (Array CGH) with Detection of Gene Dosage

Nicholas J. Wang,[1] Dahai Liu,[1] Alexander S. Parokonny,[2] and N. Carolyn Schanen[2]

[1]Department of Human Genetics, University of California–Los Angeles, Los Angeles; and [2]Nemours Biomedical Research, Alfred I. duPont Hospital for Children, Nemours Children's Clinic, Wilmington, DE

Maternally derived duplication of the imprinted region of chromosome 15q11-q14 leads to a complex neurobehavioral phenotype that often includes autism, cognitive deficits, and seizures. Multiple repeat elements within the region mediate a variety of rearrangements, including interstitial duplications, interstitial triplications, and supernumerary isodicentric marker chromosomes, as well as the deletions that cause Prader-Willi and Angelman syndromes. To elucidate the molecular structure of these duplication chromosomes, we designed a high-resolution array comparative genomic hybridization (array CGH) platform. The array contains 79 clones that form a gapped contig across the critical region on chromosome 15q11-q14 and 21 control clones from other autosomes and the sex chromosomes. We used this array to examine a set of 48 samples from patients with segmental aneuploidy of chromosome 15q. Using the array, we were able to determine accurately the dosage, which ranged from 1 to 6 copies, and also to detect atypical and asymmetric rearrangements. In addition, the increased resolution of the array allowed us to position two previously reported breakpoints within the contig. These results indicate that array CGH is a powerful technique to study rearrangements of proximal chromosome 15q.

Introduction

Chromosome 15q11-q14 is a region highly susceptible to clinically important genomic rearrangements, including interstitial deletions, duplications, triplications, and the generation of supernumerary marker chromosomes (SMCs), called "idic" or "inverted duplication" (inv dup) chromosomes (Knoll et al. 1989; Crolla et al. 1995; Browne et al. 1997; Ungaro et al. 2001). Deletions of the region lead to Prader-Willi syndrome (PWS [MIM 176270]) and Angelman syndrome (AS [MIM 105830]), depending on the deleted chromosome's parent of origin—paternal and maternal, respectively (Knoll et al. 1989). These deletions generally occur with the use of three commonly recognized breakpoints (BP1, BP2, and BP3), whereas duplications and triplications have been described that involve two additional distal breakpoints (BP4 and BP5) (Knoll et al. 1990; Christian et al. 1995; Repetto et al. 1998; Wandstrat et al. 1998). The ~4-Mb segment that encompasses the PWS/AS critical region lies between BP2 and BP3. Each of the common breakpoints harbors transcribed END repeats that are derived from the ancestral *HERC2* locus, which is located just proximal to BP3, as well as a number of other low-copy repeat (LCR) elements (Amos-Landgraf et al. 1999; Christian et al. 1999; Pujana et al. 2002). These repeat sequences are thought to mediate misalignment of the region during meiosis, leading to unequal recombination events.

The most common type of duplication identified is the SMC(15), which can result from either an intra- or interchromosomal recombination event (Wandstrat and Schwartz 2000). These marker chromosomes range in size from tiny, largely heterochromatic chromosomes that rarely have clinical consequences to large euchromatic SMC(15) frequently associated with developmental disorders (Huang et al. 1997; Eggermann et al. 2002). Overall, ~50% of SMCs are derived from chromosome 15, with the occurrence of the marker chromosome estimated to be ~1/5,000 live births (Webb 1994; Crolla et al. 1995). Notably, duplications of chromosome 15q11-q14 also display parent-of-origin effects, with maternal duplications associated with a complex neurobehavioral phenotype that often includes autism (Cook et al. 1997; Dawson et al. 2002).

The duplications arise through aberrant recombination events often involving the same breakpoints as the PWS and AS deletions, although more distal LCR also contribute to the formation of some duplication chromosomes. These distal breakpoints are rarely involved in the deletion events, indicating that some, but not all,

Received February 23, 2004; accepted for publication May 27, 2004; electronically published June 11, 2004.

Address for correspondence and reprints: Dr. N. Carolyn Schanen, Department of Human Genetics, University of California–Los Angeles, Los Angeles, CA 90095. E-mail: schanen@medsci.udel.edu

0002-9297/2004/7502-0012$15.00

duplications arise as the reciprocal recombination product of the PWS/AS deletions (Robinson et al. 1998). Moreover, recent data indicate heterogeneity of the position of the breakpoints involved in the formation of large SMC(15) chromosomes, particularly those near BP3, which appeared to be distributed across a 1.2-Mb segment, on the basis of standard cytogenetic and molecular approaches (Maggouta et al. 2003; Roberts et al. 2003).

Array comparative genomic hybridization (array CGH) has been used elsewhere to scan for genomic abnormalities at a 1-Mb resolution level, as well as at higher resolutions, for a single chromosome or smaller genomic region (Bruder et al. 2001; Hodgson et al. 2001; Vissers et al. 2003; Yu et al. 2003). The use of array CGH has been able to increase the resolution available to studies of chromosomal abnormalities from ~5 Mb, achieved by metaphase FISH, to ~100 kb, or the size of a BAC clone. A recent study that used an array of 18 genomic clones with a resolution of ~650 kb applied this strategy to the investigation of chromosome 15q11-q14. The array was able to identify rearrangements and to accurately detect copy number (Locke et al. 2004). Here, we describe the development and validation of an array CGH platform to study chromosome 15 abnormalities at a resolution of ~140 kb. This approach allows us not only to assess copy number, but to define breakpoints within the commonly rearranged region on chromosome 15q11-q14. This BAC/PAC-based genomic array improves dramatically the efficiency of evaluating the region and identifies asymmetry in the positions of the recombination events in a population of duplication chromosomes.

Material and Methods

Patient Samples

Patients carrying a duplication of chromosome 15 and cytogenetically normal parental controls were enrolled after informed parental consent with the use of protocols approved by the institutional review boards of the University of California–Los Angeles, and the Alfred I. duPont Hospital for Children. PWS cell lines GM-13566 and GM-11385 were obtained from the Coriell cell bank and had been described elsewhere as carrying deletions in the PWS critical region. Genomic DNA was isolated from lymphoblastoid cell lines or peripheral leukocytes with the PureGene DNA purification kit (Gentra), in accordance with the manufacturer's protocol.

Selection and Preparation of BAC/PAC DNA

Genomic clones chosen as targets for our array had been mapped to their chromosomal locations by FISH or by the July 2003 human reference sequence based on NCBI build 34, available at the UCSC genome browser. A gapped contig covering the known duplication region was formed by choosing overlapping clones, when possible, along with eight clones from chromosome 15 that lie outside the duplication region. There are a total of 31 gaps within our contig for which we do not have overlapping clones. Most (22 of 31) are short in length, with a range of 1–73 kb and an average of 22 kb, as determined by available sequence. Four gaps are longer, 101–255 kb, accounting for ~58% of the total region that is not represented on the array, and cluster near BP3A and BP3B.

The remaining five gaps are regions of the genome that have not yet been sequenced successfully. These gaps have been assigned a size of 100 kb each, but their actual size is unknown. Nine clones from other autosomes—seven from the X chromosome and two from the Y chromosome—also were selected as control targets. Each clone was verified by size on the basis of a *Not*I digestion run on 1% agarose pulse-field gel electrophoresis. DNA was isolated from bacterial cultures with the use of Qiagen-tip 500 columns, in accordance with standard protocols. Purified target DNA was sonicated to ~500–3,000 bp and was resuspended in 50% dimethyl sulfoxide (Sigma) with 18.5 mg/mL nitrocellulose (Millipore).

Array Printing, Blocking, and Hybridization

Target DNA was printed onto slides coated with 3-aminomethoxysilane (Sigma), by an Omnigrid 100 robot with a server arm (Genemachines) (Bruder et al. 2001). Each slide contained two array sets, with each probe printed in quadruplicate in each array. Slides were blocked in 25% formamide, 4 × saline-sodium citrate (SSC), 1% BSA (Sigma), and 0.1% SDS at 45°C for 1 h.

Test and reference genomic DNA (2 μg) were sonicated to ~500–3,000 bp, isopropanol precipitated, resuspended in dH_2O, and labeled with Cy3 or Cy5 dCTP (Amersham) by random priming with a BioPrime DNA labeling kit (Invitrogen). Unincorporated nucleotides were removed by centrifugation with the use of a Microcon YM-30 filter (Millipore). Purified labeled test and reference DNA samples were coprecipitated with 70 μg of Cot-I DNA (Invitrogen) and were resuspended in hybridization buffer containing 50% formamide, 2 × SSC, 10% dextran sulphate, 1 × Denhardt solution, 0.5 mM of EDTA, and 40 mM of sodium phosphate (pH 7). The hybridization mix was denatured at 72°C for 20 min and was incubated for 2 h at 45°C to block repetitive sequences. Slides were hybridized for 16–18 h at 45°C. For each experiment, a dye-reversed hybridization was performed on the same slide. After hybridization, cover slips were removed, and the slides were washed in 50% formamide, 2 × SSC, and 0.1% SDS for 20 min at 45°C and then in 1 × PBS for 20 min at room

temperature. Washed slides were rinsed in dH_2O and were spun dry.

Imaging and Analysis

Images were scanned using GenePix 4000B (Axon Instruments) and were analyzed using GenePixPro 4.1 (Axon Instruments). Spots were inspected visually to remove any that contained local biases. Each hybridization was analyzed individually first. Signal intensity variation between Cy5 and Cy3 was normalized by the total intensity of the non–chromosome 15 autosome spots. After normalization, the local background was subtracted from the mean intensity for each spot, and values that had a signal-to-noise ratio <5 were excluded. The $\log_2$ transformations of the test/reference (T/R) ratios were calculated, and the mean and SDs of the ratios for the four replicates within one hybridization were determined. If the SD among replicates was >0.3, the values of the replicates were inspected manually to determine the source of the variation. If a single spot gave a discordant value when compared with the others, the individual spot was discarded. If the variation reflected variability across the four replicates or if only one spot for a given clone met the criteria for inclusion, the clone was discarded and data for that clone were discarded also from the dye-reversed hybridization. The dye-reversed hybridization was subjected to the same analyses, and the overall mean and SDs of the T/R ratios for each clone that met criteria on both hybridizations were calculated. Clones that had an SD of >0.3 among replicates between hybridizations were discarded. The data were plotted versus chromosomal position. This comparison of the dye-reversed experiments allowed us to reduce greatly the likelihood of a false positive result.

The copy number results for each patient were based on a standard curve generated from our control sample results. Those clones that represented well-characterized duplications, deletions, and normals were used to create mean values for the classes of 1, 2, 3, 4, and 6 genomic copies, with means of −0.81, 0.01, 0.51, 0.90, and 1.37, respectively. To ascertain the gain/loss and copy number of the individual, $\log_2$ ratios for a given clone were taken in conjunction with the values of neighboring clones to increase the amount of information available to make an inference.

FISH Analysis

FISH analysis was performed as described elsewhere (Pinkel et al. 1988). Metaphase spreads were prepared from lymphoblastoid cell lines or phytohemagglutinin cultures of peripheral leukocytes. DNA from BAC or from cosmid clones from chromosome 15 was nick translated and was cohybridized with a centromere probe for chromosome 15 (pcm15) generously provided by Dr. Mariano Rocchi (University of Bare, Italy). The presence of a signal on a marker chromosome or of multiple spots on a chromosome 15 homolog gave evidence for duplication. Hybridization was detected by epifluorescence with the use of a Leica DM RXA2 microscope running OpenLab 3.1.3 software (Improvision). A minimum of 20 metaphase spreads was examined for each probe.

Southern Blot Analysis

Genomic DNA (2 μg) was restriction digested and separated on a 0.8% agarose gel. Transfer of the DNA onto a Hybond nylon membrane (Amersham) was performed overnight by capillary action. The membrane was prehybridized with PerfectHyb hybridization buffer (Sigma). Probes were labeled with α-^{32}P-dCTP with the use of PrimeIt II (Stratagene) and were purified across a NucTrap column (Stratagene) before application to the membrane. Hybridized membranes were washed to a stringency of 1 × SSC and 0.1% SDS. Blots were visualized on a Storm imager (Amersham) after overnight exposure on a phosphorimager cassette and were analyzed using ImageQuant (Amersham). Band intensities for test samples were compared with cytogenetically normal controls to determine copy number. Duplications and deletions were identified by either an increase or a decrease in band intensities, respectively.

Results

Preparation of the Array

Array CGH has been used widely to detect constitutional and acquired genomic rearrangements. To develop an array-CGH–based method to efficiently assess chromosomal rearrangements of chromosome 15q11-q14, including both duplications and deletions, we identified a group of genomic clones that had been mapped to our target region, either by FISH experiments or by sequencing, as target sequences to be printed onto glass arrays. A total of 79 BAC and PAC clones (see BAC/PAC Resource Center Web site) from chromosome 15 were used to create a gapped contig covering 11.6 Mb of chromosome 15 and were mapped to their locations by the July 2003 human reference sequence based on NCBI build 34, available at the UCSC genome browser (table 1). Overall, there were five gaps within our critical region that represent segments that have not yet been sequenced successfully, which were estimated at ~100 kb each (fig. 1). The exact size of these gaps is not known, however, because of the lack of reliable sequence, and three of them lie in regions that contain common breakpoint sites in chromosome 15q11-q14. In addition, our array has 26 small gaps, in which the clones do not overlap within regions that have been sequenced. Most are smaller than

Table 1

Chromosome 15q11-q14 Array Clones and Control Clones on the Array

Clone No.[a]	GenBank Accession No.	Name	Location (Mb)	Cytogenetic Band
1	AC116165	RP11-467N20	20.2	15q11.2
3	AC135069	RP11-1081C20	20.3	15q11.2
2	…	146J12	20.4	15q11.2
4	…	770C6	20.5	15q11.2
5	AC011767	RP11-26F2	20.5	15q11.2
6	AC138649	RP11-1180F24	20.7	15q11.2
7	AC025138	RP11-291O21	20.8	15q11.2
8	AC136687	RP11-439M15	20.9	15q11.2
9	…	pDJ81g20	21.1	15q11.2
10	AC073446	RP11-757E13	21.1	15q11.2
11	AC126407	RP11-73C9	21.3	15q11.2
12	…	pDJ181p7	21.4	15q11.2
13	AC103750	RP11-494F2	21.4	15q11.2
14	…	pDJ437h9	21.6	15q11.2
15	AC021439	RP11-484P15	21.6	15q11.2
16	AC087474	RP11-350A1	21.8	15q11.2
17	AC087463	RP11-682C24	22.0	15q11.2
18	AC139147	RP11-107D24	22.1	15q11.2
19	AC090983	RP11-385H1	22.3	15q11.2
20	AC006412	pDJ276C12	22.5	15q11.2
21	AC006412	pDJ121D5	22.6	15q11.2
22	AC124312	RP11-701H24	22.7	15q11.2
23	AC080077	RP11-441B20	22.8	15q11.2
24	AC100774	RP13-487P22	23.0	15q12
25	AC084009	RP13-487P22	23.1	15q12
26	AC004259	pDJ14I12	23.1	15q12
27	AC004738	pDJ351H23	23.2	15q12
28	AC124311	RP11-479F18	23.2	15q12
29	AC109512	RP11-931B1	23.4	15q12
30	AC016266	RP11-2C7	23.6	15q12
31	AC044913	RP11-446P9	23.7	15q12
32	AC100836	RP11-1084I9	23.8	15q12
33	AC012060	RP11-19A24	23.9	15q12
34	AC080121	RP13-500A21	23.9	15q12
35	AC103969	RP11-876F5	24.0	15q12
36	AC023840	RP11-560A2	24.2	15q12
37	AC022603	RP11-20B10	24.2	15q12
38	AC011196	RP11-48J4	24.3	15q12
39	AC104569	RP11-147D1	24.5	15q12
40	AC135999	RP13-911E13	24.6	15q12
41	AC011224	RP11-10K20	24.6	15q12
42	AC131310	RP11-150C6	24.7	15q12
43	AC006602	pDJ476i9	24.8	15q12
44	…	pDJ69i9	24.8	15q12
45	AC019229	RP11-570N16	24.9	15q12
46	AC104002	RP11-100M12	25.3	15q12
47	AC026087	RP11-595N10	25.6	15q12
48	AC124091	RP11-640H21	25.7	15q13.1
49	AC126332	RP11-665A22	26.0	15q13.1
50	AC138749	RP11-536P16	26.4	15q13.1
51	AC127522	RP13-126C7	26.9	15q13.1
52	AC016484	RP11-18H24	27.2	15q13.1
53	AC011827	RP11-57H1	27.3	15q13.1
54	AC102941	RP11-300A12	27.5	15q13.1
55	AC022613	RP11-680F8	27.7	15q13.1
56	AC087455	RP11-143J24	27.8	15q13.2
57	AC120045	RP11-932O9	28.0	15q13.2
58	AC135731	RP11-261B23	28.2	15q13.2
59	AC019322	RP11-382B18	28.3	15q13.2
60	AC111164	RP11-1109N12	28.5	15q13.2
61	AC135989	RP11-800O12	28.6	15q13.2
62	AC023151	RP11-736I24	28.7	15q13.2
63	AC087481	RP11-540B6	28.8	15q13.2
64	AC009562	RP11-348B17	29.0	15q13.3
65	AC012236	RP11-16E12	29.2	15q13.3
66	AC009873	RP11-126J9	29.4	15q13.3
67	AC021316	RP11-11J16	29.4	15q13.3
68	AC026951	RP11-456J20	29.7	15q13.3
69	AC079969	RP11-636P14	29.8	15q13.3
70	AC068448	RP11-624A21	30.1	15q13.3
71	AC139426	RP13-395E19	30.2	15q13.3
72	AC135983	RP11-632K20	30.4	15q13.3
73	AC124094	RP11-1203N1	30.6	15q13.3
74	AC074201	RP11-758N13	30.7	15q13.3
75	AC018870	RP11-88O16	30.8	15q13.3
76	AC019278	RP11-12O16	31.0	15q13.3
77	…	184n23	31.2	15q13.3
78	AC055874	RP11-489D6	31.2	15q13.3
79	AC010809	RP11-3D4	31.7	15q14
80	AC012651	RP11-164J13	40.3	15q15.1
81	AC018900	RP11-198M11	45.7	15q21.1
82	AL357835	RP11-426M11	11.8	1p36.22
83	AC016768	RP11-560C7	23.1	2p24.1
84	AC104662	RP11-660M5	24.9	4p15.2
85	…	RP11-595N1	12.1	4q27
86	AC010677	RP11-660I4	26.0	7p15.2
87	AL133410	RP11-112J3	35.7	9p13.3
88	AC020654	RP11-496H24	36.4	12q11
89	AC023449	RP11-345J18	55.7	12q13
90	AC010533	RP11-229O3	64.7	16q21
91	AL353698	RP13-238N7	55.0	Xp11.21
92	AL354793	RP11-431N15	55.5	Xp11.21
93	AL157698	RP13-188A5	64.3	Xq12
94	…	P-F19743	153.3	Xq28
95	…	P-O21668	153.3	Xq28
96	…	P-B231028	153.3	Xq28
97	…	P-K191192	153.4	Xq28
98	AC053490	RP11-140H23	24.1	Yq11.223
99	AC068123	RP11-88F4	49.7	Yq12
100[b]	…	…	…	…

[a] Corresponds to clone numbers used in figure 4.
[b] Spot number 100 is blank.

30 kb and do not present a large obstacle for accurate measurements. On the basis of available sequences, we have ~92% coverage over the 11.6-Mb region. Notably, we did not extend our contig into the repetitive sequences in the pericentromeric region of chromosome 15, which has been shown to be widely polymorphic in the population (Ritchie et al. 1998). A total of 21 targets were used as controls, including clones from other autosomes, both sex chromosomes, and a negative control.

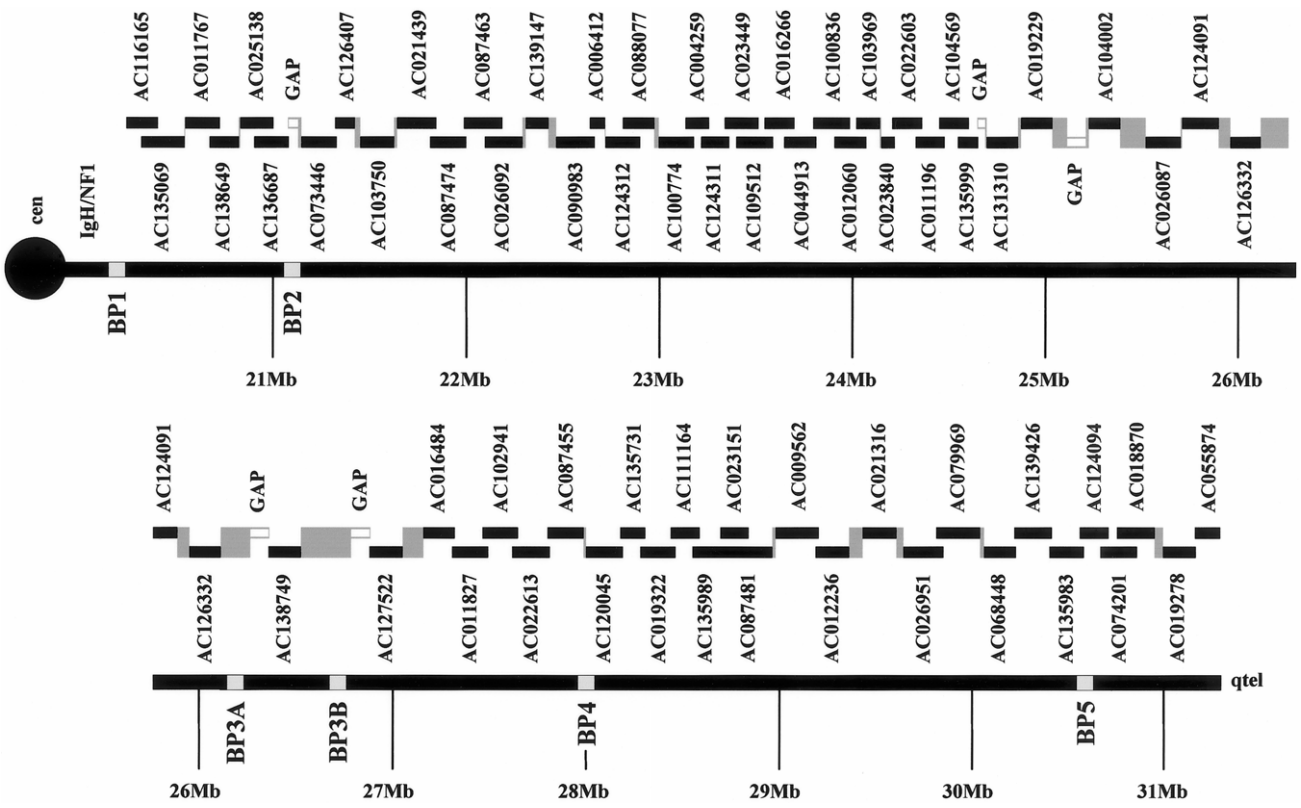

Figure 1 Gapped contig of the clones spotted on the array covering chromosome 15q11-q14. Black bars signify locations of designated clones on chromosome 15q11-q14, and gray bars/boxes represent sequenced regions not represented on the array. Unblackened boxes indicate gaps in the genomic sequence where no clones have been placed. The relative positions of the known breakpoints are indicated. Array clones derived from non–chromosome 15 autosomes, sex chromosomes, and P1 FISH clones are not shown.

Validation of the Array

We initially hybridized DNA from five pairs of cytogenetically normal controls and did not detect any labeling bias in any individual clone (fig. 2*A*). To verify gains or losses and to remove aberrant signals, the data from both dye-swap experiments were combined. The use of two experiments for each sample allowed us to remove clones that were not consistent across both experiments and that might have led to inaccurate dosage estimates. The normalized mean $\log_2$ ratio for these samples was 0.01 ± 0.08 (95% CI 0–0.02). It is of note that in these control experiments, we detected some variation in the $\log_2$ ratios for clones surrounding BP2 and BP3. These breakpoints have high homology to each other, as well as to the ancestral *HERC2* gene. It is likely that this variation is a result of repetitive elements or of polymorphisms in the number of duplicons present in each locus.

To validate the chromosome 15 array, as a means to detect segmental rearrangements of the region, we then tested the array with the use of samples from 13 patients with well-characterized chromosomal rearrangements of chromosome 15q11-q14. All 13 patients had been studied previously by the use of standard molecular techniques (table 2). Each sample was analyzed first by FISH to determine the presence and type of duplication. After verification of the presence of a duplication, a minimum of five clones were used as FISH probes to detect the extent of duplications on a metaphase chromosome spread. Further analysis of dosage was done on the basis of quantitative Southern blot analysis using 6–10 single-copy probes from chromosome 15q11-q14. Samples were also genotyped with 20 STS markers from chromosome 15q11-q14, for evidence of a duplication. The presence of three alleles at a given STS was used to determine not only the extent of the duplication but also the parent of origin. On the basis of methylation analyses using the *SNRPN* exon-α probe and of genotyping, all of the duplication chromosomes arose through an illegitimate recombination event in the maternal germline.

The group of patients chosen as dosage controls represented the spectrum of possible chromosomal abnormalities that have been seen in this region. The deletion in the PWS cell line GM-11385 (Kubota et al. 1996)

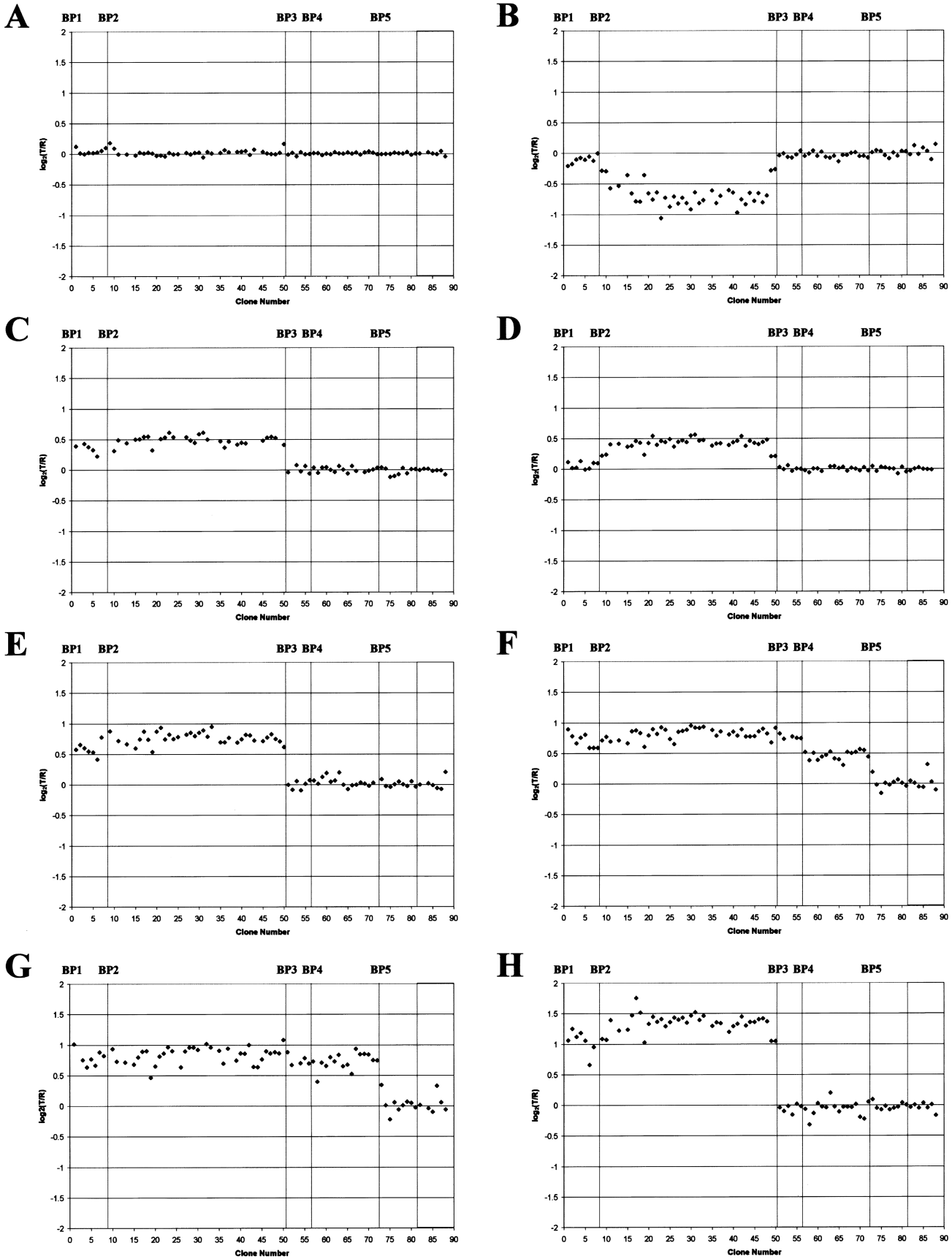
A
B
C
D
E
F
G
H
BP1
BP2
BP3
BP4
BP5
log2(T/R)
Clone Number

was detected as a decrease in the $\log_2$ ratio to an average of -0.81 ± 0.09 (95% CI -0.86 to -0.76) (fig. 2*B*). The region of decreased dosage extended from AC126407 (spot 11) to AC126332 (spot 49), corresponding to known breakpoints for this sample (BP2:BP3A). To determine the signal generated by trisomy for the region, we hybridized DNA from four patients with interstitial duplications—two patients carrying a BP1:BP3 duplication and two patients carrying a BP2:BP3 duplication. Consistent with the results of our molecular and cytogenetic analyses, all four patients were found to have duplications that extended through BP3B, and we were able to resolve the differences in proximal breakpoints (fig. 2*C* and 2*D*). The average $\log_2$ T/R ratio of clones from these duplicated regions was 0.51 ± 0.12 (95% CI 0.48–0.52).

To determine whether we could detect the difference between trisomy and tetrasomy, we hybridized DNA from six patients carrying different forms of SMC(15) (fig. 2*E*–2*G*). When we compared the $\log_2$ T/R ratios of interstitial duplications, we were able to see an increase in signal from the samples carrying an SMC(15), with an average $\log_2$ ratio of 0.90 ± 0.17 (95% CI 0.88–0.91) for clones from the regions known to be tetrasomic. In the SMC(15) samples, we also were able to detect the use of four different distal breakpoints. The smallest SMC(15) was identified in a patient with AS and paternal uniparental disomy. The SMC(15) arose from a symmetric BP2:BP2 recombination that did not lead to duplication of the PWS/AS region. Markers of this size have been reported elsewhere and usually are not associated with a phenotype, although they can be seen occasionally in patients with PWS or AS. For this case, methylation analysis, genotyping, and dosage were consistent with paternal uniparental disomy. Four patient samples showed symmetric marker chromosomes, with two arising from a BP3:BP3 recombination and two arising from a BP5:BP5 event. Two patients were found to carry an asymmetric marker chromosome with a BP4:BP5 junction. Although we did not have samples from patients who are pentasomic for the region, two patients have been identified who carry large tricentric SMC(15), leading to partial hexasomy for chromosome 15q11-q13 (Mann et al., in press). Hybridization of these samples to the array led to a further increase in the signal, with an average $\log_2$ ratio of 1.37 ± 0.15 (95% CI 1.32–1.41) (fig. 2*H*).

Using the data from the 18 control hybridizations, we generated a standard curve that demonstrates a strong correlation ($R^2 = 0.99$) between the $\log_2$ T/R ratio and dosage (fig. 3). The measured ratios approximated the theoretical values, and the means (± 1 SD) were not overlapping for dosages from one to four copies. However, there was some overlap of values between four and six copies. This is expected, since the use of the $\log_2$ transformation of the ratios leads to a flattening of the predicted values at higher log values, and the relative differences in copy number are smaller.

Detection and Mapping of Breakpoint Sites

To map the five breakpoints to clones on our array, we used data from previous studies, in addition to data generated from our control samples, to position the breakpoints. BP1, BP2, and BP3 were described first in the formation of PWS/AS deletions, whereas BP4 and BP5 were identified later, on the basis of their involvement in the formation of large SMC(15)s (Christian et al. 1999; Pujana et al. 2002). The position and orientation of the three proximal breakpoints, BP1–BP3, are well characterized; thus, the clones that flank them could be predicted on the basis of sequence data (Christian et al. 1995, 1999). The most centromeric clone on the array (AC116165 [spot 1]) lies just telomeric to BP1 and shows increased dosage in duplications involving BP1 (fig. 2). Similarly, the clones flanking BP2 (AC136687 and AC073446 [spots 8 and 10]), BP3A (AC126332 and AC138749 [spots 49 and 50]), and BP3B (AC138749 and AC127522 [spots 50 and 51]) were distinguished easily on the array, on the basis of consistent transitions in the $\log_2$ T/R ratio in our control patient samples (fig. 2*B*–2*E*).

Since the two distal breakpoints, BP4 and BP5, have not been characterized fully, the arrays were able to provide additional information about the positions of these elements. BP4 was identified initially in a patient with an intrachromosomal triplication and was mapped, within ~1.2 Mb, in the interval between markers D15S1019 and D15S165, which are contained in clones AC011827 (spot 53) and AC087481 (spot 63), respec-

Figure 2 The $\log_2$ T/R ratio plots for control samples representing various forms of segmental rearrangements of chromosome 15q11-q14. *A,* Cytogenetically normal control. *B,* Patient GM-11385 with PWS and a BP2:BP3A deletion. *C,* Interstitial duplication event between BP1 and BP3B, leading to trisomy in patient 98-19. *D,* Interstitial duplication between BP2 and BP3A, leading to trisomy in patient 99-9. *E,* Supernumerary SMC(15) with a BP3B:BP3B junction in patient 03-71, leading to tetrasomy for the involved regions. *F,* SMC(15) with an asymmetric BP4:BP5 junction in patient 99-70. *G,* SMC(15) with a BP5:BP5 junction in patient 99-73. *H,* SMC(15) resulting in partial hexasomy of chromosome 15q11-q14 in patient 00-29. In the plots, only the clones representing chromosome 15q11-q14 are shown. A ratio >0.3 indicated a gain of DNA copy number for the clone, whereas a ratio <−0.3 indicated a loss of DNA copy number. The vertical lines represent the locations of breakpoints, as determined by our array analysis and by published reports. BP3A is not shown but lies between spots 49 and 50.

Table 2

Molecular Analysis of Control Duplication Samples

			Results of								
			FISH				Southern Blot				
Cell Line	Duplication Type	Breakpoint Class	CEN pcm15	BP1:BP2 770C6	BP2:BP3 437H9	BP3:BP4 204M06	BP1:BP2 pCS-1540	BP2:BP3 pCS-9991	BP3:BP4 pCS-APBA2	BP4:BP5 pCS-39528[a]	Methylation
98-19	Interstitial	BP1:BP3B	+	+	+	−	2.7	3.1	2.1	…	Maternal
00-33[b]	Interstitial	BP1:BP3B	+	+	+	−	4.3	4.3	1.9	…	Maternal
99-9	Interstitial	BP2:BP3B	+	−	+	−	2.2	3.3	1.8	…	Maternal
01-12	Interstitial	BP2:BP3B	+	−	+	−	2.1	3.1	2.0	…	Maternal
01-30	Marker	ptel:BP2:BP2:ptel	+	+	−	−	3.6	2.2	1.7	…	Loss of maternal
01-16	Marker	ptel:BP3B:BP3B:ptel	+	+	+	−	4.2	3.6	2.1	…	Maternal
02-18	Marker	ptel:BP3B:BP3B:ptel	+	+	+	−	3.8	4.1	1.9	…	Maternal
99-70	Marker	ptel:BP4:BP5:ptel	+	+	+	+	4.1	3.8	3.9	2.6	Maternal
02-7	Marker	ptel:BP4:BP5:ptel	+	+	+	+	4.1	3.9	4.2	3.2	…
99-73	Marker	ptel:BP5:BP5:ptel	+	+	+	+	4.2	4.1	4.2	4.1	Maternal
99-89	Marker	ptel:BP5:BP5:ptel	+	+	+	+	4.2	4.1	3.6	3.6	Maternal
98-22	Marker	ptel:BP3B:BP3B:ptel:ptel:BP3B:BP3B:ptel	+	+	−	−	4.7	5.9	1.7	…	Maternal
00-29	Marker	ptel:BP3B:BP3B:ptel:ptel:BP3B:BP3B:ptel	+	+	−	−	5.1	6.4	1.7	…	Maternal

[a] Patients who showed no evidence by FISH or by proximal Southern blot for carrying duplications distal to BP3 were not probed with pCS-39528.

[b] Patient carries an interstitial triplication.

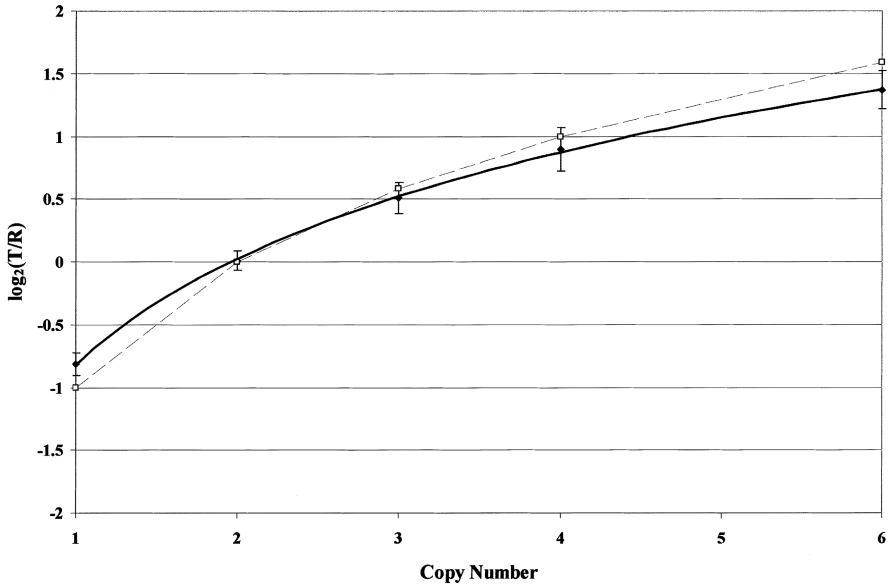

Figure 3 Standard curve of $\log_2$ T/R ratios. The observed ratios for each copy number are represented by blackened squares (± 1 SD), with a corresponding trend line. The gray dashed line represents theoretical values at a given copy number (*gray diamonds*).

tively (Ungaro et al. 2001). BP5 was mapped previously within the YAC 810f11, just proximal to D15S1010 (Wandstrat and Schwartz 2000). D15S1010 is contained by clone AC074201 (spot 74) on our array. On the basis of the array results, it appears that BP4 is contained within the genomic region defined by clones AC087455 (spot 56) and AC120045 (spot 57), which places it just distal to D15S1043 (fig. 2*F*). BP5 appears to lie within clone AC124094 (spot 73), since the $\log_2$ ratio value for AC124094 was consistently intermediate to the proximal duplicated clones and to the distal clones that showed normal dosage in duplication chromosomes involving this breakpoint (fig. 2*F*–2*G*). The intermediate value suggests that the sequences in this clone are duplicated only partially in rearrangements involving BP5.

Since BP5 represented the distal boundary of the duplication in several samples, we confirmed the placement of BP5 on SMC(15) by FISH analysis with clone AC124094 and with an overlapping telomeric clone, AC074201. Signals for both clones were detected on the normal chromosome 15 homologs. Only the clone AC124094 hybridized to the SMC(15) (fig. 4). The signal generated from the marker chromosome was consistently weaker than those on the normal homologs, which is consistent with partial duplication of the clone. In addition, a faint signal was detected distally (15q24), in a region known to share homology with 15q11-q14 (Pujana et al. 2002). This homology would be predicted to contribute to an intermediate signal intensity on the array.

Analysis of a Patient Sample Set

After validation of our array and the identification of the clones that represent breakpoint positions, we assessed an additional 35 patients with the use of array CGH (fig. A1 [online only]). These patients carried known duplication chromosomes and included 4 patients with interstitial rearrangements and 31 patients with SMC(15). Each had been characterized partially by FISH, Southern blot, and genotyping. We used the standard curve values to assign dosage in the patient sample.

Each of the four interstitial duplication cases (02-12, 02-20, 02-21, and 02-22) was trisomic for the interval between BP1 and BP3 (table 3), and two primary classes of SMC(15) were detected, as well as two cases with atypical rearrangements. The most frequent form of SMC(15) that we observed included 18 samples with an apparently asymmetric recombination event between BP4 and BP5. This led to tetrasomy for the interval from BP1 through BP4 and to trisomy from BP4 to BP5 in 16 of 18 cases (breakpoint class ptel:BP4:BP5:ptel) (table 3). The relative frequency of this form of asymmetric SMC(15) suggests that recombination between BP4 and BP5 is the predominant mechanism of formation of large SMC(15)s that extend distal to BP3.

The second largest class of SMC(15) included 13 SMC(15)s that involved a BP3B:BP3B recombination event distal to clone AC138749 (spot 50). AC138749 lies distal to BP3A and proximal to BP3B, as reported elsewhere (Christian et al. 1999) (fig. 2). The absence of cases showing a recombination event proximal to

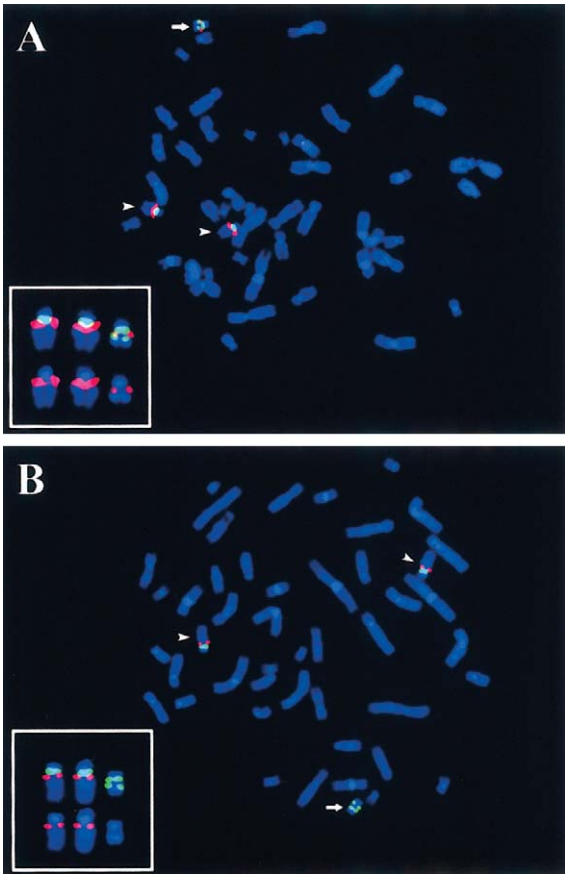

Figure 4 Mapping of BP5 by metaphase FISH of patient 03-28. Chromosome 15 homologs are marked by an arrowhead, and the SMC(15) is marked by an arrow. Enlargements of the images are inset, with the top row showing dual color hybridization and the bottom-row red signal arising from the BAC clone. *A*, Red signals represent clone AC124094 (spot 73), and green signals represent pcm15 (chromosome 15 centromere). Hybridization of AC124094 is seen on the normal homologs and on the SMC(15), with a weaker signal on the SMC(15). *B*, Red signals represent AC074201 (spot 74), and the green signals represent pcm15. Clone AC074201 hybridizes to the normal chromosome 15 homologs but not to the SMC(15). These data place the breakpoint within clone AC124094, which is consistent with its intermediate fluorescence signal on the array.

AC138749, among our SMC(15) cases, indicates that BP3B is the predominant recombination site in the formation of an SMC(15). We did not identify any additional cases involving a symmetric BP5:BP5 recombination in our sample population.

An exchange between BP4 and BP5 was involved in the generation of the SMC(15) in the two atypical cases (99-36 and 00-3); however, these samples showed $\log_2$ T/R ratio values consistent for trisomy, rather than tetrasomy, for a number of clones in the BP1:BP2 region (fig. *5A–5B*). To assess the basis of the apparent inconsistencies in dosage across the interval, FISH experiments were performed with clones 770c6 (spot 4), AC011767 (spot 5), AC138649 (spot 6), AC025138 (spot 7), and AC136687 (spot 8). These studies revealed a deletion on one copy of chromosome 15 in the sample from patient 00-3. This deletion included clones 770c6 and AC011767, although distal clones AC138649, AC025138, and AC136687 were present on both chromosome 15 homologs (fig. *5C–5D*). Patient 99-36 showed evidence for only one copy of clones AC011767 and AC138649 but showed two copies for clones AC025138 and AC136687, as well as two centromere signals on the marker chromosome (fig. *5E–5F*).

Discussion

Array CGH is an emerging technique being used to generate high-resolution analysis of copy-number variation and breakpoint analysis. It has been applied extensively in cancer cytogenetics to investigate acquired abnormalities in tumor cell lines, but it has been used also to scan the genome for cryptic constitutional rearrangements or to investigate specific regions that are prone to deletion or duplication (Bruder et al. 2001; Buckley et al. 2002; Veltman et al. 2002; Vissers et al. 2003; Yu et al. 2003). In this report, we describe an array CGH platform that allows efficient analysis of deletions and duplications of chromosome 15q11-q14, with ~92% coverage. Our results expand on data from a lower-resolution chromosome 15 array CGH platform that recently was reported to detect duplications and deletions of proximal 15q (Locke et al. 2004). We characterized our array with the use of a group of dosage controls derived from patients with well-defined duplications and deletions of chromosome 15q11-q14 that ranged from segmental monosomy to hexasomy and found that we could reliably distinguish dosages between one and six copies. We then applied this approach to the broader group of patients with known duplication chromosomes, including both interstitial duplications and SMC(15)s.

Classes of Duplications and Asymmetry

Our arrays were able to detect two classes of interstitial duplications and five classes of SMC(15) duplications, as well as a BP2:BP3 interstitial deletion. These chromosomal abnormalities were confirmed further by FISH, Southern blots, and microsatellite data (see Genome Database Web site for microsatellite markers). SMC(15)s have been shown to be heterogeneous in their genomic content (Mignon et al. 1996; Wandstrat et al. 1998; Roberts et al. 2003). Our array was able to detect five classes of SMC(15) with the use of the common breakpoints within 15q11-q14. The two most frequent duplication classes in our patient sample involved a BP3B:BP3B recombination (13/31 patients) or a BP4:

Table 3

Array CGH Analysis of Duplication Samples

Cell Line	Duplication Type	Breakpoint Class[a]	No. of Copies for Interval (Probes)[b]					
			CEN-BP1 (pcm15)	BP1-BP2 (AC116165-AC136687)	BP2-BP3B (AC073446-AC138749)	BP3B-BP4 (AC127522-AC087455)	BP4-BP5 (AC120045-AC124094)	BP5-TEL (AC124094)
02-12	Interstitial	BP1:BP3B	2	3	3	2	2	2
02-20	Interstitial	BP1:BP3B	2	3	3	2	2	2
02-21	Interstitial	BP1:BP3B	2	3	3	2	2	2
02-22	Interstitial	BP1:BP3B	2	3	3	2	2	2
98-17	idic(15)	ptel:BP3B:BP3B:ptel	4	4	4	2	2	2
99-23	idic(15)	ptel:BP3B:BP3B:ptel	4	4	4	2	2	2
99-47	idic(15)	ptel:BP3B:BP3B:ptel	4	4	4	2	2	2
00-5	idic(15)	ptel:BP3B:BP3B:ptel	4	4	4	2	2	2
01-19	idic(15)	ptel:BP3B:BP3B:ptel	4	4	4	2	2	2
03-17	idic(15)	ptel:BP3B:BP3B:ptel	4	4	4	2	2	2
03-23	idic(15)	ptel:BP3B:BP3B:ptel	4	4	4	2	2	2
03-34	idic(15)	ptel:BP3B:BP3B:ptel	4	4	4	2	2	2
03-37	idic(15)	ptel:BP3B:BP3B:ptel	4	4	4	2	2	2
03-46	idic(15)	ptel:BP3B:BP3B:ptel	4	4	4	2	2	2
03-67	idic(15)	ptel:BP3B:BP3B:ptel	4	4	4	2	2	2
03-71	idic(15)	ptel:BP3B:BP3B:ptel	4	4	4	2	2	2
03-74	idic(15)	ptel:BP3B:BP3B:ptel	4	4	4	2	2	2
99-10	idic(15)	ptel:BP4:BP5:ptel	4	4	4	4	3	2
99-27	idic(15)	ptel:BP4:BP5:ptel	4	4	4	4	3	2
99-78	idic(15)	ptel:BP4:BP5:ptel	4	4	4	4	3	2
99-86	idic(15)	ptel:BP4:BP5:ptel	4	4	4	4	3	2
99-93	idic(15)	ptel:BP4:BP5:ptel	4	4	4	4	3	2
01-8	idic(15)	ptel:BP4:BP5:ptel	4	4	4	4	3	2
01-22	idic(15)	ptel:BP4:BP5:ptel	4	4	4	4	3	2
01-25	idic(15)	ptel:BP4:BP5:ptel	4	4	4	4	3	2
01-33	idic(15)	ptel:BP4:BP5:ptel	4	4	4	4	3	2
02-4	idic(15)	ptel:BP4:BP5:ptel	4	4	4	4	3	2
02-9	idic(15)	ptel:BP4:BP5:ptel	4	4	4	4	3	2
03-4	idic(15)	ptel:BP4:BP5:ptel	4	4	4	4	3	2
03-10	idic(15)	ptel:BP4:BP5:ptel	4	4	4	4	3	2
03-28	idic(15)	ptel:BP4:BP5:ptel	4	4	4	4	3	2
03-40	idic(15)	ptel:BP4:BP5:ptel	4	4	4	4	3	2
03-43	idic(15)	ptel:BP4:BP5:ptel	4	4	4	4	3	2
99-36	idic(15)	ptel:BP4:BP5:ptel	4	3	4	4	3	2
00-3	idic(15)	ptel:BP4:BP5:ptel	4	3	4	4	3	2

[a] Breakpoint classes were verified by genotyping, FISH, and Southern blot analysis.
[b] Copy numbers were verified by quantitative Southern blots.

BP5 recombination (18/31 patients) event. These data agree with a report involving large SMC(15)s, in which the patient sample set contained 14/46 patients with a possible BP3:BP3 recombination and 32/46 samples showed a larger asymmetric recombination event (Roberts et al. 2003). Although the authors described possible heterogeneity for their BP3 recombination site, they were not able to make a conclusive statement because of the lack of resolution by metaphase FISH. Our array data were able to determine that BP3B was used preferentially in the formation of the BP3:BP3 SMC(15), resulting in the generation of a symmetrical supernumerary derivative chromosome 15. The most common duplication type that we encountered was an asymmetric ptel:BP4:BP5:ptel SMC(15). Similarly, Roberts et al. (2003) identified the asymmetric use of breakpoints in formation of markers in their study, with BP5 as the distal breakpoint, although they located the other breakpoint close to BP3. The comprehensive data generated from our array studies support their conclusion of an asymmetric SMC(15) population; however, we did not detect any rearrangements arising from a BP3:BP5 exchange. In contrast, we were able to refine the location of the breakpoint to within ~100 kb surrounding the telomeric end of AC087455 and the centromeric end of AC120045, indicating that it is most likely BP4 (Ungaro et al. 2001; Pujana et al. 2002). All cases of asymmetry involved these two distal breakpoints. The other three classes of SMC(15) were detected in our control sample set but were not identified in our patient sample set. These

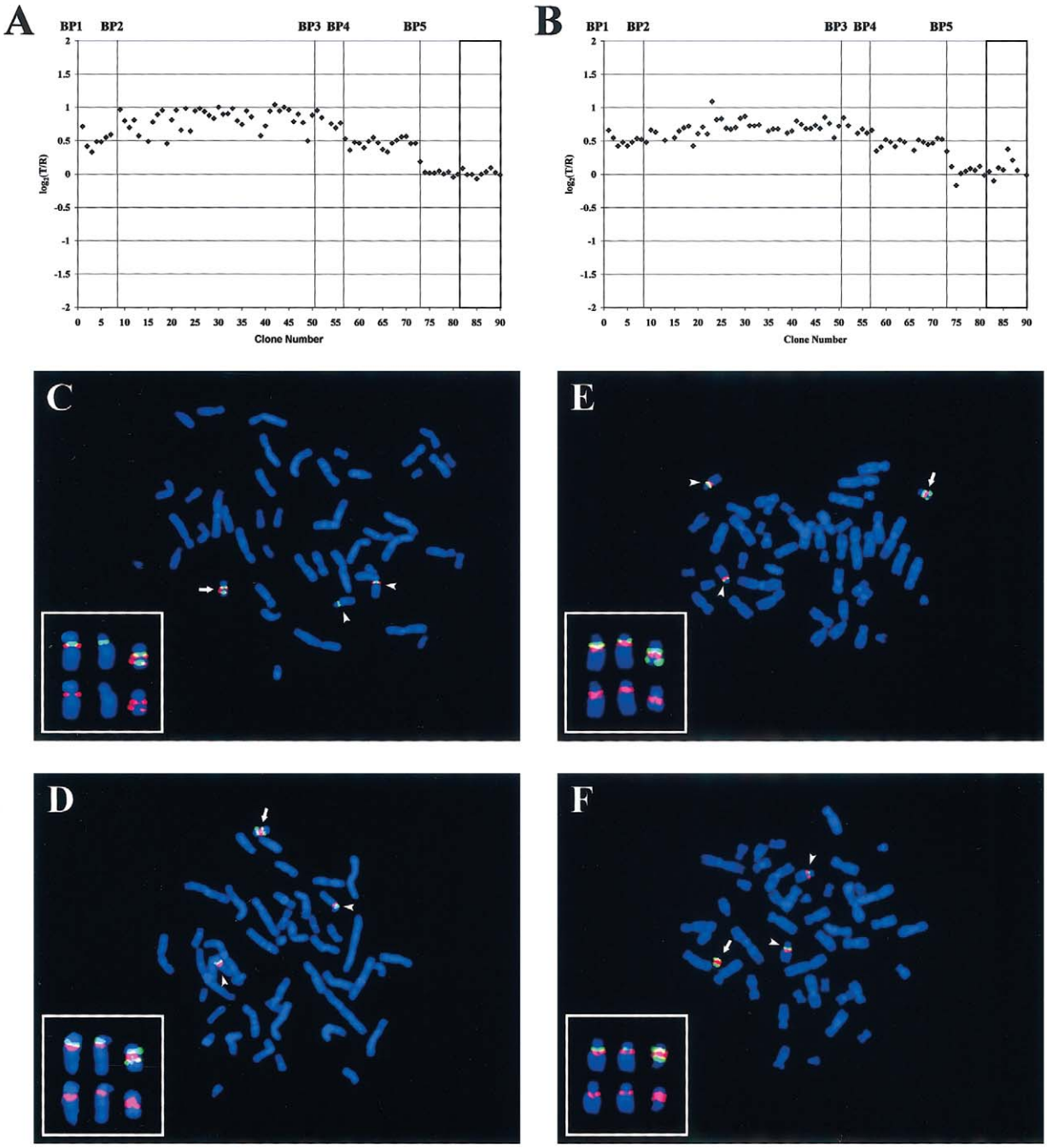

Figure 5 Characterization of deletions in patients 00-3 and 99-36 by FISH. Array data charts for 00-3 (*A*) and 99-36 (*B*) show a relative decrease in signal intensity for clones in the interval between BP1 and BP2. *C,* FISH analysis of the BP1–BP2 interval, with clone AC011767 (spot 5, *red*) and with pcm15 (*green*). The absence of hybridization of clone AC011767 to one chromosome 15 homolog in metaphase spreads from patient 00-3 was consistently detected, although two paired signals were present on the SMC(15). *D,* FISH with clone AC138649 (spot 6, *red*) and with pcm15 (*green*) on metaphase chromosomes from patient 00-3. Signals for the more telomeric clone, AC138649, were present on both chromosome 15 homologs. *E,* FISH with clone AC138649 (spot 6, *red*) and with pcm15 (*green*) on metaphase chromosomes from patient 99-36. The presence of a single paired signal on the SMC(15) for clone AC138649 indicates that there is only one copy of the region. *F,* FISH with a more distal clone, AC138687 (spot 8, *red*), and with pcm15 (*green*) generating a double signal from clone AC138687, consistent with two copies on the idic(15). *C–F*, Arrowheads indicate chromosome 15 homologs; arrows indicate the SMC(15). Enlargements of the images are inset, with the top row showing dual color hybridization and the bottom-row red signal arising from the BAC clone.

included two BP5:BP5 SMC(15)s, two tricentric SMC(15)s, and a single case involving a small SMC(15) derived from a BP2:BP2 recombination.

It is notable that we did not detect any SMC(15) derived from any other potential combinations of breakpoints, such as BP2:BP4 or BP2:BP5. Although a BP1:BP1 SMC(15) has been reported elsewhere (Huang et al. 1997), the absence of duplications involving other breakpoint pairs suggests some specificity, in that the types and positions of recombination events that give rise to SMC(15) most likely result from sequence homology and orientation.

Atypical Cases

Four atypical duplications were identified in this group of patients, including two cases with partial hexasomy and two cases with trisomy for the region proximal to BP2. Two of these cases, 98-22 and 00-29, carry tricentric SMC(15)s that contain four copies of all duplicated regions (Mann et al., in press). Data from these microarray experiments validate earlier data that these extremely large SMC(15) contain four additional copies of genomic material through BP3. Partial hexasomy of the PWS/AS critical region has been seen in other patients, occurring as a result of a large SMC(15) or the presence of multiple SMC(15)s (Maggouta et al. 2003; Nietzel et al. 2003; Qumsiyeh et al. 2003).

The duplications found in patients 99-36 and 00-3 were not only asymmetric for the BP4:BP5 region but were also trisomic for material proximal to BP2, suggesting a complex rearrangement. Recently, four genes have been mapped to chromosome 15 between BP1 and BP2 (Chai et al. 2003). *CYFIP1*, *GCP5*, *NIPA1*, and *NIPA2* are highly conserved genes in vertebrates with orthologs in invertebrates. Although the deletion sizes differ between 00-3 and 99-36, the four known genes are predicted to be deleted in both cases. Though these genes are not imprinted, they are considered candidate modulators of the PWS/AS phenotype (Butler et al. 2004). Smaller SMC(15)s that do not carry extra genomic material distal to BP2 but that do carry copies of these four genes are not associated with an abnormal phenotype (Huang et al. 1997). Thus, although these two patients are trisomic and not tetrasomic for the region, it is unlikely that this will have a discernable effect on their phenotype.

Breakpoint Mapping

Electronic content mapping of the genomic clones allows distinction of the clones that flank previously mapped breakpoints (BP1–BP3), whereas a transition in $\log_2$ T/R ratio values has allowed us to map two breakpoints described elsewhere that had not been fully mapped (BP4 and BP5). Our localization of breakpoints involved in chromosome 15q11-q14 rearrangements, by array CGH, is in agreement with all previous mapping efforts and, in the case of BP4 and BP5, refines their location to within ~100–200 kb. On the basis of NCBI build 34 of the human genome sequence, there is inverted sequence homology between a region telomeric to BP4 in clone AC019322 (spot 59) and a region centromeric to BP5 in clone AC068448 (spot 70), resulting in two locations for a number of markers, including D15S937 and RH39597. The mechanism for the formation and presence of these two distal breakpoints may lie in the shared homology that results in illegitimate pairing during meiosis, and the inverted orientation may underlie the generation of the SMC(15).

Applications of Array CGH

We have used array CGH as a high-resolution high-throughput method to study duplications of chromosome 15q11-q14. Other studies of these duplications have relied on FISH, Southern blot analysis, and genotyping to define duplication sizes. Our array was able to expand data generated from these standard molecular methods, to determine size and copy number of these duplications as well as location of breakpoints, allowing for more efficient analysis. Although these other techniques are useful in determining interstitial versus SMC(15) rearrangements, as well as parent of origin and methylation status, array CGH will allow a robust and efficient way to determine the extent of the duplication. Moreover, the increased resolution of array CGH provides a powerful approach to detect small atypical duplications or deletions in the region.

Our array CGH platform will allow for the efficient analysis of small duplications and deletions within chromosome 15q11-q14 in patients with developmental disorders for whom no cytogenetic abnormality has been detected. This technique provides a powerful tool for a systematic examination of a complex genomic region with links to multiple neurodevelopmental disorders.

Acknowledgments

We are very grateful to the patient families and the Iso-Dicentric 15 Exchange, Advocacy, and Support (IDEAS) group for participating in our study and to Naghmeh Dorrani for coordinating patient enrollment. We thank Barb Malone, Dianne York, and Suzanne Mann for technical assistance. We are grateful to David Ledbetter, Judy Fantes, Roger Schultz, Mariano Rocchi, and Anne-Marie Poustka for generously providing genomic clones. We would like to thank Christina Zheng for her assistance with figure preparation. This study was supported by grants from the National Institutes of Health Collaborative Programs for Excellence in Autism (NIH-U19-HD-35470), Nemours, and the F & F Foundation.

Electronic-Database Information

URLs for data presented herein are as follows:

BAC/PAC Resources Center, http://bacpac.chori.org (for BAC and PAC clones)
Genome Database, http://www.gdb.org (for microsatellite markers)
Online Mendelian Inheritance in Man (OMIM), http://www.ncbi.nlm.nih.gov/Omim/
UCSC Genome Browser, http://genome.ucsc.edu (for clone positions)

References

Amos-Landgraf JM, Ji Y, Gottlieb W, Depinet T, Wandstrat AE, Cassidy SB, Driscoll DJ, Rogan PK, Schwartz S, Nicholls RD (1999) Chromosome breakage in the Prader-Willi and Angelman syndromes involves recombination between large, transcribed repeats at proximal and distal breakpoints. Am J Hum Genet 65:370–386

Browne CE, Dennis NR, Maher E, Long FL, Nicholson JC, Sillibourne J, Barber JC (1997) Inherited interstitial duplications of proximal 15q: genotype-phenotype correlations. Am J Hum Genet 61:1342–1352

Bruder CE, Hirvela C, Tapia-Paez I, Fransson I, Segraves R, Hamilton G, Zhang XX, et al (2001) High resolution deletion analysis of constitutional DNA from neurofibromatosis type 2 (NF2) patients using microarray-CGH. Hum Mol Genet 10:271–282

Buckley PG, Mantripragada KK, Benetkiewicz M, Tapia-Paez I, Diaz De Stahl T, Rosenquist M, Ali H, et al (2002) A full-coverage, high-resolution human chromosome 22 genomic microarray for clinical and research applications. Hum Mol Genet 11:3221–3229

Butler MG, Bittel DC, Kibiryeva N, Talebizadeh Z, Thompson T (2004) Behavioral differences among subjects with Prader-Willi syndrome and type I or type II deletion and maternal disomy. Pediatrics 113:565–573

Chai JH, Locke DP, Greally JM, Knoll JH, Ohta T, Dunai J, Yavor A, Eichler EE, Nicholls RD (2003) Identification of four highly conserved genes between breakpoint hotspots BP1 and BP2 of the Prader-Willi/Angelman syndromes deletion region that have undergone evolutionary transposition mediated by flanking duplicons. Am J Hum Genet 73: 898–925

Christian SL, Fantes JA, Mewborn SK, Huang B, Ledbetter DH (1999) Large genomic duplicons map to sites of instability in the Prader-Willi/Angelman syndrome chromosome region (15q11-q13). Hum Mol Genet 8:1025–1037

Christian SL, Robinson WP, Huang B, Mutirangura A, Line MR, Nakao M, Surti U, Chakravarti A, Ledbetter DH (1995) Molecular characterization of two proximal deletion breakpoint regions in both Prader-Willi and Angelman syndrome patients. Am J Hum Genet 57:40–48

Cook EH Jr, Lindgren V, Leventhal BL, Courchesne R, Lincoln A, Shulman C, Lord C, Courchesne E (1997) Autism or atypical autism in maternally but not paternally derived proximal 15q duplication. Am J Hum Genet 60:928–934

Crolla JA, Harvey JF, Sitch FL, Dennis NR (1995) Supernumerary marker 15 chromosomes: a clinical, molecular and FISH approach to diagnosis and prognosis. Hum Genet 95: 161–170

Dawson AJ, Mogk R, Rothenmund H, Bridge PJ (2002) Paternal origin of a small, class I inv dup(15). Am J Med Genet 107:334–336

Eggermann K, Mau UA, Bujdoso G, Koltai E, Engels H, Schubert R, Eggermann T, Raff R, Schwanitz G (2002) Supernumerary marker chromosomes derived from chromosome 15: analysis of 32 new cases. Clin Genet 62:89–93

Hodgson G, Hager JH, Volik S, Hariono S, Wernick M, Moore D, Nowak N, Albertson DG, Pinkel D, Collins C, Hanahan D, Gray JW (2001) Genome scanning with array CGH delineates regional alterations in mouse islet carcinomas. Nat Genet 29:459–464

Huang B, Crolla JA, Christian SL, Wolf-Ledbetter ME, Macha ME, Papenhausen PN, Ledbetter DH (1997) Refined molecular characterization of the breakpoints in small inv dup(15) chromosomes. Hum Genet 99:11–17

Knoll JH, Nicholls RD, Magenis RE, Glatt K, Graham JM Jr, Kaplan L, Lalande M (1990) Angelman syndrome: three molecular classes identified with chromosome 15q11q13-specific DNA markers. Am J Hum Genet 47:149–155

Knoll JH, Nicholls RD, Magenis RE, Graham JM Jr, Lalande M, Latt SA (1989) Angelman and Prader-Willi syndromes share a common chromosome 15 deletion but differ in parental origin of the deletion. Am J Med Genet 32:285–290

Kubota T, Aradhya S, Macha M, Smith AC, Surh LC, Satish J, Verp MS, Nee HL, Johnson A, Christan SL, Ledbetter DH (1996) Analysis of parent of origin specific DNA methylation at SNRPN and PW71 in tissues: implication for prenatal diagnosis. J Med Genet 33:1011–1014

Locke DP, Segraves R, Nicholls RD, Schwartz S, Pinkel D, Albertson DG, Eichler EE (2004) BAC microarray analysis of 15q11-q13 rearrangements and the impact of segmental duplications. J Med Genet 41:175–182

Maggouta F, Roberts SE, Dennis NR, Veltman MW, Crolla JA (2003) A supernumerary marker chromosome 15 tetrasomic for the Prader-Willi/Angelman syndrome critical region in a patient with a severe phenotype. J Med Genet 40:e84

Mann SM, Wang NJ, Liu DH, Wang L, Schultz RA, Dorrani N, Sigman M, Schanen NC. Supernumerary tricentric derivative chromosome 15 in two boys with intractable epilepsy: another mechanism for partial hexasomy. Hum Genet (in press)

Mignon C, Malzac P, Moncla A, Depetris D, Roeckel N, Croquette MF, Mattei MG (1996) Clinical heterogeneity in 16 patients with inv dup 15 chromosome: cytogenetic and molecular studies, search for an imprinting effect. Eur J Hum Genet 4:88–100

Nietzel A, Albrecht B, Starke H, Heller A, Gillessen-Kaesbach G, Claussen U, Liehr T (2003) Partial hexasomy 15pter→15q13 including SNRPN and D15S10: first molecular cytogenetically proven case report. J Med Genet 40:e28

Pinkel D, Landegent J, Collins C, Fuscoe J, Segraves R, Lucas J, Gray J (1988) Fluorescence in situ hybridization with human chromosome-specific libraries: detection of trisomy 21 and translocations of chromosome 4. Proc Natl Acad Sci USA 85:9138–9142

Pujana MA, Nadal M, Guitart M, Armengol L, Gratacos M,

Estivill X (2002) Human chromosome 15q11-q14 regions of rearrangements contain clusters of LCR15 duplicons. Eur J Hum Genet 10:26–35

Qumsiyeh MB, Rafi SK, Sarri C, Grigoriadou M, Gyftodimou J, Pandelia E, Laskari H, Petersen MB (2003) Double supernumerary isodicentric chromosomes derived from 15 resulting in partial hexasomy. Am J Med Genet 116:356–359

Repetto GM, White LM, Bader PJ, Johnson D, Knoll JH (1998) Interstitial duplications of chromosome region 15q11q13: clinical and molecular characterization. Am J Med Genet 79:82–89

Ritchie RJ, Mattei MG, Lalande M (1998) A large polymorphic repeat in the pericentromeric region of human chromosome 15q contains three partial gene duplications. Hum Mol Genet 7:1253–1260

Roberts SE, Maggouta F, Thomas NS, Jacobs PA, Crolla JA (2003) Molecular and fluorescence in situ hybridization characterization of the breakpoints in 46 large supernumerary marker 15 chromosomes reveals an unexpected level of complexity. Am J Hum Genet 73:1061–1072

Robinson WP, Dutly F, Nicholls RD, Bernasconi F, Penaherrera M, Michaelis RC, Abeliovich D, Schinzel AA (1998) The mechanisms involved in formation of deletions and duplications of 15q11-q13. J Med Genet 35:130–136

Ungaro P, Christian SL, Fantes JA, Mutirangura A, Black S, Reynolds J, Malcolm S, Dobyns WB, Ledbetter DH (2001) Molecular characterisation of four cases of intrachromosomal triplication of chromosome 15q11-q14. J Med Genet 38:26–34

Veltman JA, Schoenmakers EF, Eussen BH, Janssen I, Merkx G, van Cleef B, van Ravenswaaij CM, Brunner HG, Smeets D, van Kessel AG (2002) High-throughput analysis of subtelomeric chromosome rearrangements by use of array-based comparative genomic hybridization. Am J Hum Genet 70:1269–1276

Vissers LE, de Vries BB, Osoegawa K, Janssen IM, Feuth T, Choy CO, Straatman H, van der Vliet W, Huys EH, van Rijk A, Smeets D, van Ravenswaaij-Arts CM, Knoers NV, van der Burgt I, de Jong PJ, Brunner HG, van Kessel AG, Schoenmakers EF, Veltman JA (2003) Array-based comparative genomic hybridization for the genomewide detection of submicroscopic chromosomal abnormalities. Am J Hum Genet 73:1261–1270

Wandstrat AE, Leana-Cox J, Jenkins L, Schwartz S (1998) Molecular cytogenetic evidence for a common breakpoint in the largest inverted duplications of chromosome 15. Am J Hum Genet 62:925–936

Wandstrat AE, Schwartz S (2000) Isolation and molecular analysis of inv dup(15) and construction of a physical map of a common breakpoint in order to elucidate their mechanism of formation. Chromosoma 109:498–505

Webb T (1994) Inv dup(15) supernumerary marker chromosomes. J Med Genet 31:585–594

Yu W, Ballif BC, Kashork CD, Heilstedt HA, Howard LA, Cai WW, White LD, Liu W, Beaudet AL, Bejjani BA, Shaw CA, Shaffer LG (2003) Development of a comparative genomic hybridization microarray and demonstration of its utility with 25 well-characterized 1p36 deletions. Hum Mol Genet 12:2145–2152